Differential structural organization and gene expression regulatory networks of lamin A Ig fold domain mutants of muscular dystrophy.

Subarna Dutta[1,2] ,Vikas Kumar [3] , Madavan Vasudevan[2] ,

1 Department of Biochemistry,University of Calcutta , 35, Ballygunge circular road , Kolkata-700019.West Bengal. India

2 Theomics International Private Limited.28, Income Tax Layout, Sadananda Nagar, NGEF Layout, Bengaluru – 560038.India

3 University of Nebraska Medical Center.Omaha, NE 68198-5875

Correspondence :

suborna.dutta@gmail.com, madavan@theomics.com, vikas.kumar@unmc.edu.

Abstract :

In metazoan cells, lamins form a proteinaceous meshwork as major structural component of nucleus and also involve in the regulation of essential cellular processes. Lamins along with their interactors act as determinants for chromatin organization throughout the nucleus. Major dominant missense mutations for autosomal dominant forms of muscular dystrophies are resided in the Ig fold domain of lamin A. How lamin A constitutes the distribution of heterochromatin and euchromatin balance, relocates the epigenetic marks in shaping of chromatin states are currently not well defined to make any conclusion about the prognosis of lamin A mediated muscular dystrophies. In the first part of this report, we identified in-vitro organization of full length lamin A proteins due to two well cited Ig LMNA mutations : R453W, W514R by biophysical and electron microscopy observations . We further show both lamin A/C mutant cells were mainly expressed as nucleoplasmic aggregates with reduced amounts at the nuclear envelope.Labelling of specific markers of epigenetics such as H3K9me3,H3K27me3, H3K36me3,Hp1α permitted the correlation of lamin A mutations on epigenetic mechanism. Both immunofluorescence and biochemical analyses are believed to exercise a transcriptional upregulation. Beside the manipulation on epigenetic mechanism , using proteomic studies we trace diverse expressions of transcription regulators, protein components of RNA synthesis and processing, protein translation and posttranslational modification. These data suggests a severe perturbation of targeting of other proteins on

nucleus. Our study also portends specific structural configurations of lamin A determined by patterns of it's interacting partners.

Main Text:

Introduction:

Nucleus is the most rigid entity of the cell, which is separated from the cytoplasm by a double membrane system of the nuclear envelope (Dingwell C .1992). Outer nuclear membrane and inner nuclear membrane, an array of nuclear pore complex and dense near tetragonal networks of the lamina are the major structural components of the nuclear envelope. The dense tetragonal networks of intermediate filaments are generally formed due to separated but overlapping admission of lamin proteins. In vertebrates, lamin genes are expressed as one A- type lamin and two B- type lamins with a molecular weight of 65-70 kDa. The prelamin forms of each type are subjected to post-translational modifications for their respective mature forms (Adam et al. 2013, Maske et al. 2003,Dominici et al. 2009). Lamin carries tripartite structure of type-V intermediate filament, that mainly assembles with N terminal head domain(1-32 amino acids) , helical rod domain (33-383 amino acids) and C terminal globular tail domain (383-645 amino acids) (Bertrand AT et al. 2020, Strelkov SV et al. 2004, Dhe-Paganon S et al. 2002 , Dutta S et al. 2018, Krimm I et al.2002,). The longest domain among the entire protein , the alpha- helical rod domain has coiled-coil heptad -repeat pattern of three alpha-helical segments (coil 1A, coil 1B and coil 2) and short intermediate sub-domains (L1 and L 12)(Ahn et al.2019).The C terminal tail domain has an distinct immunoglobulin-like (Ig) fold domain for chromatin binding, the nuclear localization signal (NLS) for the transportation of lamin into the cell nucleus and (except the lamin C) a cys-aliphatic-aliphatic-any residue box (CAAX) (Ahn et al. 2013,Corrigan et al. 2005,Sinesky et al. 1994). The Ig-fold domain mainly consists a compact β-sandwich of nine β-strands with short loops to reside in two β-sheets (Dhe-Paganon et al. 2002). The rod domain and part of the short head region facilitate the assembly of lamins (Heitlinger et al. 1992, Isobe et al. 2007).The parallel/unstaggered alpha helical coiled-coil dimers of lamin A/C converted into high-order filamentous structures of 3.5 nm (unlike intermediate filament) with a distinct repeat of Ig fold for 20 nm intervals by lateral and longitudinal mixing (Koster et al., 2015, Parry, Strelkov et al., 2007,Turgay et al., 2017). Lamin A got it's significance due to involvement in the 500 autosomal dominant mutations ,that are associated with 16 tissue specific degenerative diseases. Most of the mutations are associated with the myopathies . Ig fold carries maximum no. of mutations of laminopathies

and among the total muscular dystrophy mutation subjects 45% are caused by this domain. The LMNA associated muscular dystrophy can be characterized by progressive skeletal muscle loss, skeletal and heart muscle weakness with cardiac dysrhythmias and cardiomyopathy(Tan D et al. 2015). Based on the phenotypes like herniation or misshapen nuclei with the destabilised structure of lamins, failure mechanism in some cellular processes like-nucleoskeleton-cytoskeleton coupling, protein-protein interactions, chromatin tethering, transcription machinery etc. two hypotheses are well accepted to define the pathogenesis of lamin A/C associated diseases. The structural hypothesis is based on the poor mechanical integrity of lamin in maintaining nuclear homeostasis. The gene regulation hypothesis points to chromatin compartmentalization and epigenetics in gene expression regulation in tissue -specific lamin A/C diseases.

Lamin A has major roles in nuclear processes like- chromatin organization and positioning, DNA replication, transcription ,gene expression (Dechat et al. 2008, Malhas et al. 2007,Tang et al. 2008) . Lamin B1stays in a close-knit with the chromatin along the nuclear periphery, whereas, lamin A cross-link chromatin throughout the nucleus directly or indirectly by histone proteins (Melcer S et al.2012, Prokocimer M et al.2009, Moir RD et al. 2000). LMNA -/- results in chromatin rearrangement as well as lamina deformation. Gene relocation at the nuclear periphery has been assigned by A-type lamins, which may provide insight into the transcriptional pathway.DNA adenine methyltransferase identification (DamID) studies showed genomic regions that are linked to lamin i.e. Lamina associated domain (LADs)(Guelen et al. 2008,Meuleuman et al. 2013, Peric-Hupkes et al. 2010,Pickersgill et al. 2006, van Steensel and Kind.2014, Kind et al. 2015) are repressive histone post-translational modifications (PTMs) enriched, gene-poor and possesses low transcription activity (de Laat W et al.2008, Yao J et al. 2017, van Steensel B et al. 2013). The lamin binding proteins and DNA-bridging proteins namely LBR, Emerin, BAF, histone, LAP2α, LAP2β associate the connection of chromatin and nuclear lamina (Mattout-Drubezki and Gruenbaum 2003, Dorner et al. 2007 , Schirmer and Foisner 2007, Worman et al. 1990, Ye and Worman 1994,1996, Foisner and Gerace 1993, Furukawa et al. 1997, Schumaker et al. 2001, Holaska et al. 2003). Lamin A/C regulates Histone Methyl Transferases by modulating pRb signalling pathways (Djabali et al. 2010, Bracken et al. 2003, Nielsen et al. 2001,Dorner et al. 2007). The analysis of LMNA mutations for FPLD,HGPS,AD-EDMD patients evince the anomaly in peripheral heterochromatin significantly (Sabatelli et al. 2001, Capanni et al. 2003, Filesi et al.2005, Lombardi et al. 2007, Goldman et al. 2004, Columbaro et al. 2005). Emerging reports in the

field consolidate the influence of distinct pattern of epigenetic landscape on heterochromatic changes in the mutated and lamin A null cells (Gonzalez Suarez I, Grotsky et al. 2009; Shumaker DK, Erdos MR 2006). Constitutive heterochromatin is defined by trimethylated histone H3 at Lys9, histone H4 at Lys 20 (H4K20me3), and histone H3 at K27 (H3K27me3), while facultative heterochromatin is defined by histone H3 at K27 (H3K27me3) (Sarma and Reinberg 2005, Martin and Zhang 2005). Lamin A/ C deficiency induces loss of heterochromatin-euchromatin ratio with the rearrangement of HP1β and H3K9 methylation (Filesi et al .2005; Galiova et al. 2008). In HGPS fibroblasts , downregulation of HP1 α along with dislocalization from H3K9me3 sites, downregulation of H3K9me3 and H3K27me3 were observed along with the upregulation of H4K20me3 (Scaffidi and Misteli 2005,Shumaker et al. 2006,Columbaro et al. 2005, Scaffidi and Misteli 2005, Shumaker et al. 2006). Old individuals expressing LAΔ50/progerin and Mandibuloacral dysplasia fibroblasts mediate anomaly in H3K9me3 level and loss of H3K27me3 (Filesi et al. 2005, Scaffidi and Misteli 2006). H3K4 methylation was reduced in C2C12 cells due to overexpression of wild type lamin A, and H3K4 hypermethylation on the MYOG promoter was lost in muscular dystrophy (R453W lamin mutation) cells, according to P Collas et al. (2008). There are several lines of evidence in support of role of lamin A level in transcriptional regulation, because condensed chromatin structure imposes perturbation in the transcription initiation by RNA Pol II (Misteli T et al. 2009, Workman J L et al. 2007). Dominant negative construct of lamin A perturbs RNA polymerase II and localization of TATA binding protein (TBP) (Kumaran et al. 2002). ΔNLA mutant (deletion of N terminal domain) transfection in BHK 21 cells showed decrease in BrUTP incorporation , which suggests dysregulation in transcription (Spann et al. 2002). On the other hand,overexpression of lamin A/C imparts loss of RNA pol II activity in HeLa cells (Kumaran et al. 2002) . These reports are semblance of impact of lamin A in the chromatin organization and regulation from gene expression to gene activity. Additionally, transcriptional activity inevitably reflects the RNA metabolism and protein metabolism(McCracken S et al.1997, Shuman, S et al. 1997 , Hirose, Y et al.1998). Interestingly, enhanced level of RNA processing (including mRNA splicing process via spliceosome process),RNA transport ,protein translation, ribosome biogenesis are observed in HGPS derived fibroblast cell (Buchwalter A et al. 2017) .Splicing factors are found to be associated with lamin A (Spann et al. 2002, Kumaran et al. 2002, Depreux FF et al.2015).

Our study offers investigation of epigenetic mechanism underlying chromatin organization and proteome profile of global gene expression regulatory network in lamin A associated

muscular dystrophy. Based on their severity two severe mutations of muscular dystrophy were studied : R453W ,W514R respectively. By proteomics approach we mapped out levels of expression of regulators behind epigenetic state, RNA synthesis and processing , protein synthesis and processing respectively. In addition to providing new information on the association of proteins , a systematic investigation of lamin A interactors was expounded.This study is also designed to give additional insights into the structural environment of full length protein due to single point mutation in the Ig fold domain of lamin A and their probable effect on their binding affinity, transcription. Our result also support alterations in heterochromatin protein distribution and RNA pol II functioning to predict gene expression patterns.

Results :

Mutation affects gel like behaviour of lamin A and the secondary structure :

Lamin provides ample support to the nucleus as lamin A deficiency results in fluid like deformation in irreversible manner (Pajerowski JD et al. 2007) . *LMNA* gene mutations disturb the nuclear compliance with the reduced chromatin stability but it's effect varies upon different single amino acid substitution(Zwerger M et al.2013, Earle AJ et al. 2020) .More recently , Banerjee A et al. 2013 and Mukherjee CM et al. 2021showed differential rheological properties in the different point mutations associated with dilated cardiomyopathy. So, it is tempting to speculate that Ig fold mutations , that are used in this study , will show variable elastic properties . We therefore tested effect of constant oscillatory shear of strain amplitude(γ) 1% at an angular frequency (ω) of 5 rad/s for 1000 sec on the viscoelastic nature of wild type and mutant proteins at .6 mg/ml concentration (**Figure 1-b**). W514R lamin showed more solid-like nature compared to wild type lamin as we got higher storage moduli (G'). Whereas, R453W lamin has consistent lower storage moduli (G') than the native protein. Interestingly, we observed higher saturation level in storage moduli(G') and loss moduli (G") for wild type lamin, which confirms stable tertiary structure. Different values of storage moduli (G') for R453W lamin and W514R lamin demonstrates disparity in polymerization population and insufficient load support as well as force transmission in various manner. Variability in viscoelastic properties might have reflected assembly patterns of lamin A. Our scanning electron microscopy data (**Figure 1-c**) showed ,W514R lamin has a preponderance to form bundled filaments with less visible cross linking when compared with the dense cross-linked network by the wild type lamin, which directly dictates strain hardening behaviour of protein.Though, R453W lamin attributes weak network formation with less bundles and cross

links. Anomaly in criss-cross density of mutant proteins was in excellent agreement with complex viscosity plot, which showed that, for W514R it is higher than that of the wt LA and for R453W lamin it is lower than that of wild type lamin A.

Change in viscoelastic properties and assembly patterns due to mutations can be understand by investigating the secondary structure of proteins i.e. from the behaviour of rod domain. Interestingly from CD spectroscopy analysis , we found non-overlapping spectra among the mutants and native protein. These alterations also suggests difference in the oligomerization status of the proteins. mutants induced elevated magnitudes of [θ] compared to the Wt in their oligomerized forms, indicating enhanced and/or altered homopolymerization. We calculated the θ222/θ208 ratio increased for W514R(~1.2) ,which confirms more coiled-coil formation due to self association of the mutant lamin A monomers; for R453W(~.89), this parameter decreased . Thus, pointing to altering helicities of LA to different extent with mutations .

θ222/ θ208 ratios are displayed in Table 1. When the ratio exceeds 1 it defines existence of coiled -coils.

Table 1 :

Proteins	**[θ]222/[θ] 208**
Wt LA	**.91**
R453W LA	**.89**
W514R LA	**1.2**

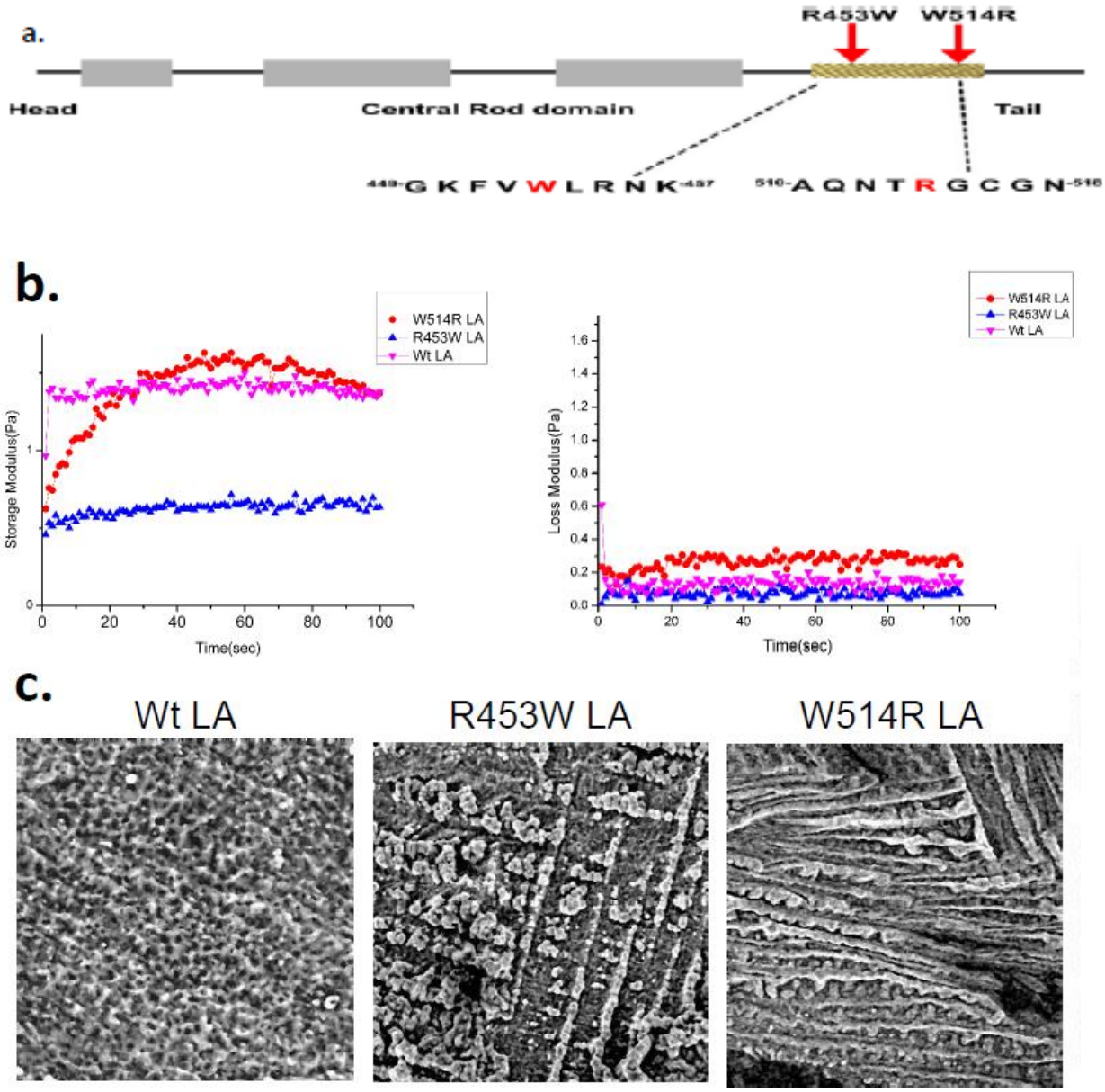

Figure 1: Structural perturbation due to lamin A mutation. (a) Represents position of two mutations in Ig fold of lamin A. (b) Viscoelastic spectra (G'> G") of lamin A changed due to muations.(c) Differential bundle –like networks and crisscross density in muscular dystrophy causing mutants compared to Wt LA by scanning electron microscopy. Scale bar = 20µm ,magnification 3000x. (d) CD spectra will be uploaded shortly.

Alteration of histone modification marks as a sequel to lamin A mutations :

Several experimental evidences suggested that histone modification marks play a role in lamin A mutations (Lattanzi et al.2007, Scaffidi and Misteli 2006, Shumaker et al. 2006, Filesi et al. 2005). We looked at H3K9me3, H3K27me3 and H3K36me3 as transcription activation and repression marks in our immunofluorescence study. H3K9me3, H3K27me3, and H3K36me3 are found in heterochromatin (Kouzarides et al. 2007), while H3K36me3 is found in euchromatin (Bartova et al. 2008, Berger 2007). H3K9me3 dots showed a significant decrease. H3K9me3 dots dropped more in EGFP LA-R453W than in EGFP LA-W514R. Histone marks were found to be colocalized with the aggregates of the R453W mutation, which was unexpected. LA R453W and LA W514R are known for their aggregate formation (Roblek, Ogris et al. 2010, Dutta S, Sengupta et al. 2018). In this regard, we found larger globular dots of H3K27me3 marks in R453W LA but low counts, as well as a diffuse staining pattern of H3K27me3 marks in LA W514R. The high accumulation of H3K36me3 dots on the nucleus in mutants corroborated this observation. **Figure 2** depicts the results of these observations. Immunoblot (**Figure. 4**) of the whole cell lysate of stably expressed EGFP WT LA and mutants confirmed the findings from immunofluorescence studies, with low expression levels of H3K9me3 and H3K27me3 and high expression of H3K36me3 in mutants.

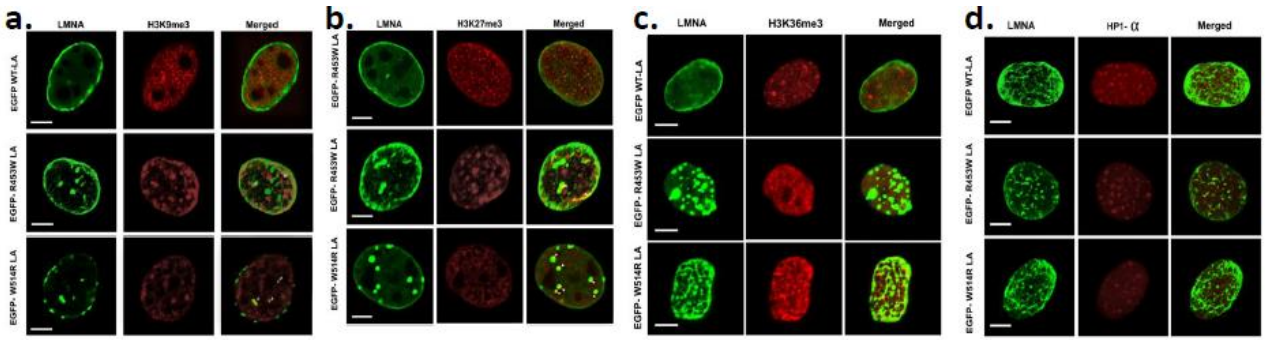

Figure 2 :Alteration of repressive epigenetic marks : H3K9 me3 (a) , H3K27me3 (b), HP1α (d) and active epigenetic mark : H3K36me3 (c) . C2C12 cells stably transfected with pEGFP WT LA, pEGFP R453W LA, pEGFP W514R LA were immunostained with anti-H3K9me3,anti-H3K27me3, anti-HP1α ,anti-H3K36me3 following counterstaining with Alexa fluor 568 .

Alteration of HP1α and dynamics in mutant lamin A:

Depletion of HP1 proteins causes a change in the genome landscape by reducing H3K9 methylation marks (Palladino F et al. 2014). High levels of HP1α are a characteristic of constitutive heterochromatin (Trojer and Reinberg, 2007). We found low recruitment of HP1α in heterochromatin foci for mutant LA in immunofluorescence studies, confirming the reduced level of H3K9me3 found in our immunofluorescence and immunoblot studies (**Figure. 2-d**). Our findings were also consistent with immunoblot results, which showed a decrease in intensity level for both LA R453W and LA W514R. (**Figure. 4**). Our findings are consistent with previous findings that showed HP1α depletion in Lamin A rod mutants (Chaturvedi, Parnaik 2010). Our findings were in line with the FRAP experiment (**Figure 3**).

Due to mutant LA, we observed high HP1α dynamics. It refers to the sequestration of HP1α recruitment on heterochromatin as a result of increased oligomeric exchange between protein molecules and, as a result, less stable complex formation with H3K9me3. Notably, from our calculation (also mentioned in **Figure 3-c**) we obtained the halftime ($t_{1/2}$) of recovery for EGFP WT LA was 5 ± 0.625 s, EGFP R453W LA was 1.8 ± 0.225s, EGFP W514R LA was 2.5 ± 0.312 s.

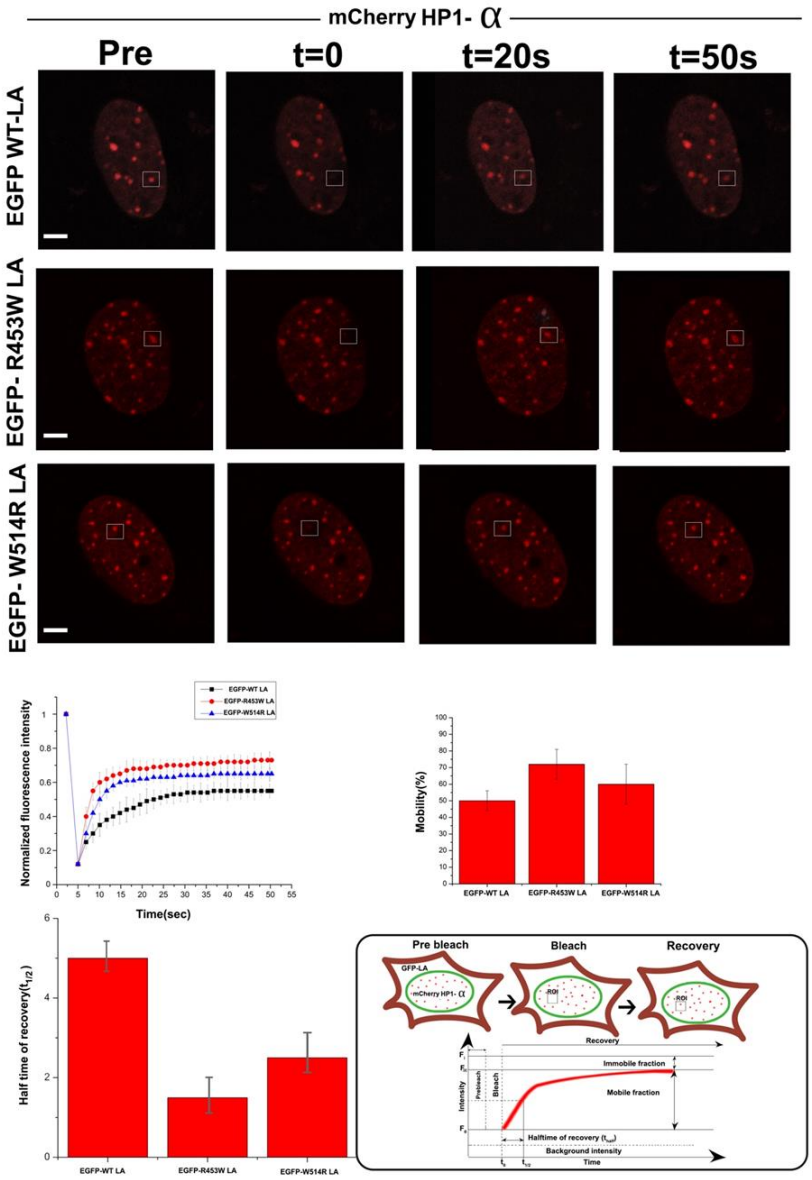

Figure 3 : Alteration of HP1α dynamics in mutant lamin A. (a). Representative time series FRAP images of mCherry-HP1α immedietly following the photobleach (t=0), Bar,10µm. C2C12 cells were transiently transfected with EGFP-WT / EGFP-R453W / EGFP W514R –mCherry HP1α for 24 hours prior to FRAP. (b). FRAP analysis of mCherry HP1α in wild type and mutants .Y axis denotes normalized florescence intensity which points percentage of recovery. (c) Half time of recovery (t1/2) graph is generated for all the samples from half maximal fluorescence recovery (F1/2). (d). Mobility graph is generated from the data obtained from normalized FRAP curves for all the samples . Data show the mean ± standard deviation for 30 cells of each sample.

Hyperactivation of RNA pol II functionality :

Several studies have suggested that lamins are involved in RNA polymerase II activity, either directly or indirectly (Timothy Spann, Robert D. Goldman 2002; Kumaran Ri et al.2002; Hessen and Fornerod 2007). The activity of RNA Pol II was disrupted in dominant negative lamin A with a terminal deletion (Spector DL et al. 2008). Phosphorylation of Serine residues in the CTD domain at positions 2,5,7 was required for RNA polymerase II activity. RNA Pol II phosphorylation at Serine 5 indicates transcription initiation (Chapman RD et al. 2008). According to immunoblot data, LA R453W had a significantly higher level of RNA Pol II s5p than LA W514R when compared to the wild type (**Figure.4**).

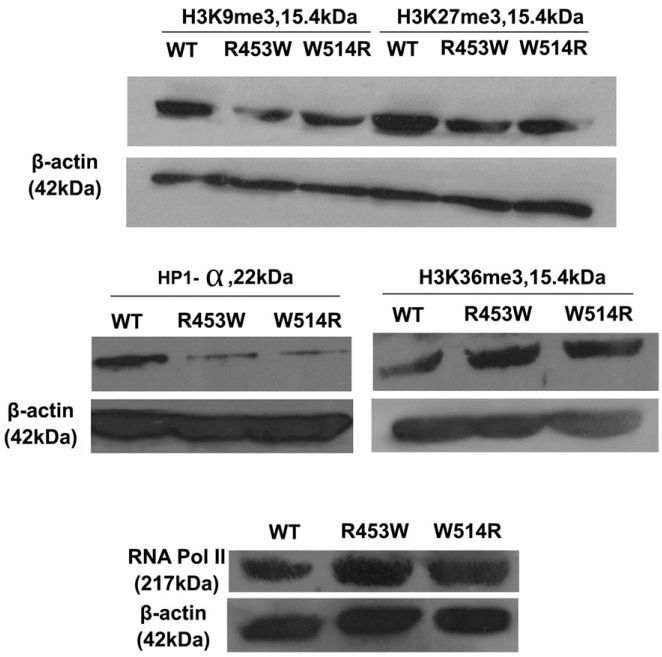

Figure 4: Cell lysates from stably transfected cells run in SDS PAGE and immunoblot with anti-H3K9me3, anti-H3K27me3, anti-H3K36me3, anti- HP1α , anti- RNA Pol II .

Proteome profile of LA mutants :

Total proteome profiling of LA R453W and LA W514R mutants were done in triplicates and wild type in duplicates. ProteinPilotTM Software 5.0(AB Sciex) was used for the protein searches .The unused value was selected in the database UniProt mouse, unused (ProtScore) for the search result (LC-MS/MS) original data, unused 1.3 was set, and a protein with a confidence level of 95 percent or more was set as the analysis target after the search was completed. In at least one of the eight samples, the resolved proteome revealed 952 proteins. Because both the mutant and the wild type had replicates, we used PCA (Principle Component

Analysis) and a Eucledian-based condition tree to determine the maximum variation across all samples and replicates (**Figure. 5**). To place the samples in specific components, PCA is plotted based on the total number of proteins expressed and their expression levels to figure out how well the biological replicates worked out. It also means that samples that are closer together have the same proteins expressed at similar levels. The condition tree is built using the distance metric, which determines how similar two samples are based on the number of proteins expressed and their expression levels. The replicate samples all clustered together, indicating very little variation. Differentially expressed proteins were determined using an Anova t-Test with a p value of 0.05 and a fold change of >=2 for a protein to be considered differentially expressed. Using the volcano plot, we discovered that LA R453W had 860 proteins upregulated and 91 proteins downregulated, while LA W514R had 392 proteins upregulated and 559 proteins downregulated. When compared to the wild type sample, unsupervised hierarchical clustering revealed overall patterns of up and down regulated proteins in both mutants.

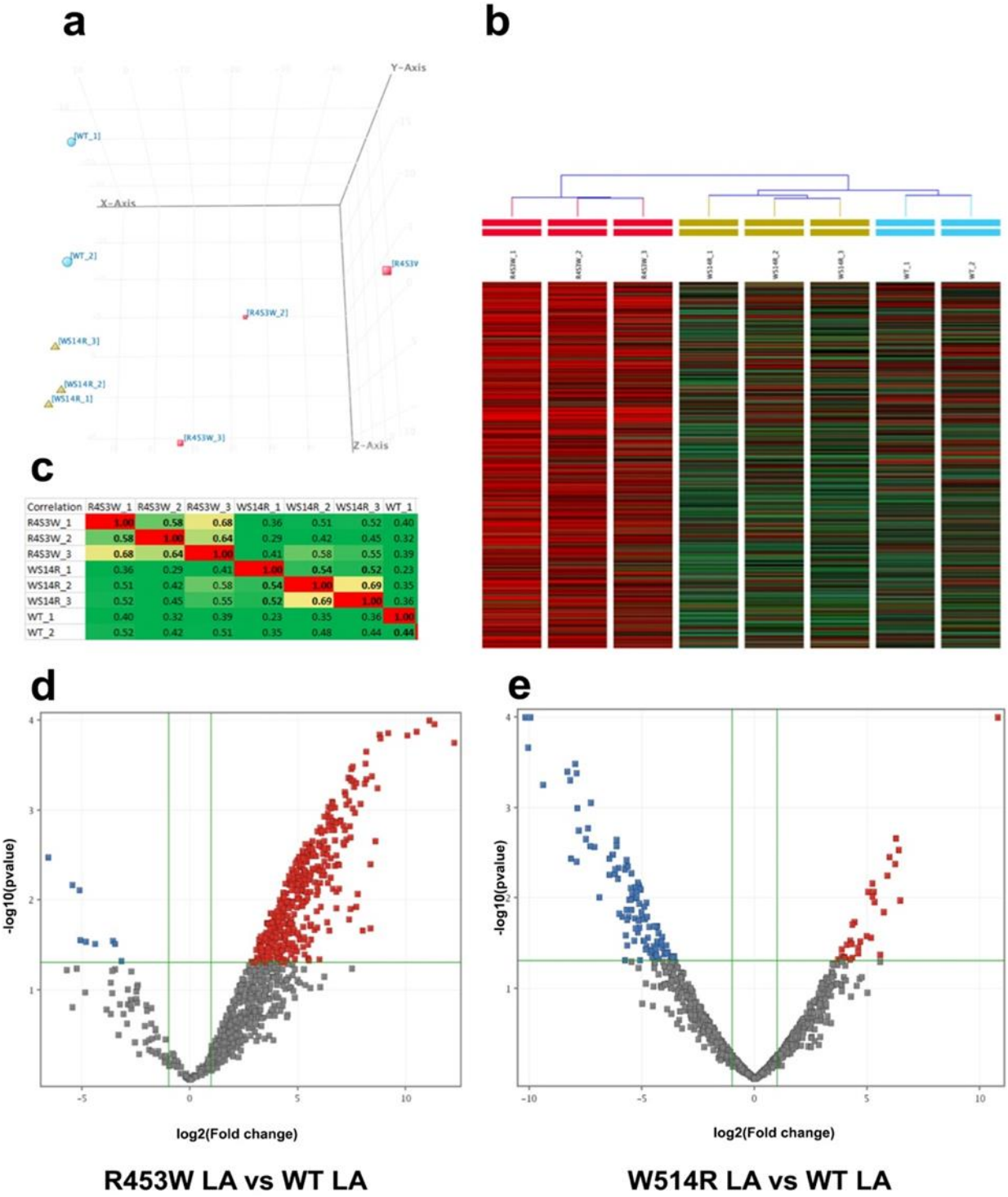

Correlation	R453W_1	R453W_2	R453W_3	W514R_1	W514R_2	W514R_3	WT_1
R453W_1	1.00	0.58	0.68	0.36	0.51	0.52	0.40
R453W_2	0.58	1.00	0.64	0.29	0.42	0.45	0.32
R453W_3	0.68	0.64	1.00	0.41	0.58	0.55	0.39
W514R_1	0.36	0.29	0.41	1.00	0.54	0.52	0.23
W514R_2	0.51	0.42	0.58	0.54	1.00	0.69	0.35
W514R_3	0.52	0.45	0.55	0.52	0.69	1.00	0.36
WT_1	0.40	0.32	0.39	0.23	0.35	0.36	1.00
WT_2	0.52	0.42	0.51	0.35	0.48	0.44	0.44

Figure 5:

Qualitative and quantitatve assessment of proteome profile :

(a), (b), (c) PCA analysis, unsupervised condition tree, correlation plot presented reproducibility among 952 proteins in at least one of the eight samples. (d),(e) volcano plots of R453W LA , W514R LA respectively. Out of 952 proteins, upregulation of 860

proteins and downregulation of 91 proteins for LA R453W and upregulation of 392 proteins and downregulation of 559 proteins for LA W514R were observed.

Quantitative assessment on gene expression regulatory proteins :

For the differentially expressed proteome, comprehensive biological functional annotations of differentially expressed proteins were performed using the Uniprot database website and DAVID data analysis software (http://david.abcc.ncifcrf.gov/home.jsp). To obtain the overall distribution of differentially expressed proteins, a genetic enrichment analysis based on Gene Ontology (GO) of biological processes, cellular components, and molecular functions was performed (**Figure supplementary 1**), which included proteins involved in epigenetic pathway, RNA synthesis and processing, protein synthesis and processing, and ribosomal proteins. The output of the GO and Pathway clusters was used as input to regulatory network modelling using in-house scripts and visualised using Cytoscape V2.8.3 to identify key nodes and edges of gene expression regulatory proteins that are uniquely dysregulated by both mutants when compared to wild type (**Figure 6**). To identify the significant functional categories and pathways, we used the p-value calculated by the hypergeometric test and corrected by FDR, with FDR 0.05 as a threshold.In our study, we have identified upregulation of 272 proteins , downregulation of 25 proteins for R453W LA sample and 141 upregulated proteins , 57 downregulated proteins for W514R LA sample among all the four selected subgroups. Regulatory proteins of protein synthesis and processing were found to be downregulated (36 proteins) in W514R LA sample.

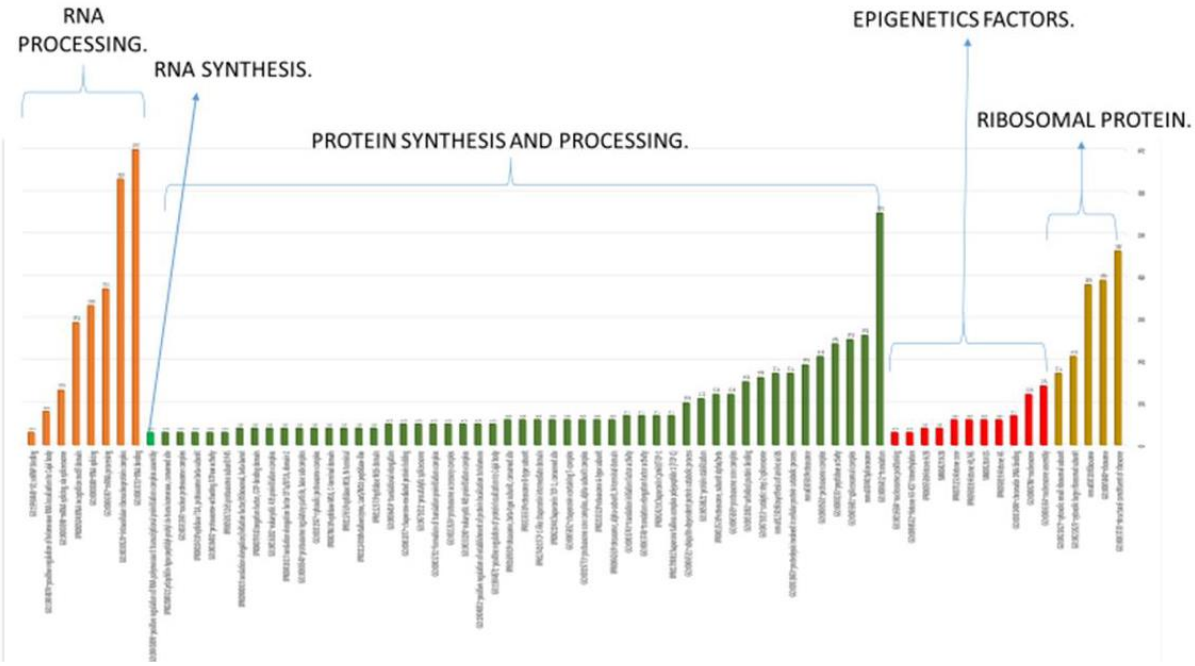

Figure supplementary 1 :

Histograms of dysregulated GO categories related to gene expression regulatory process in mutants.

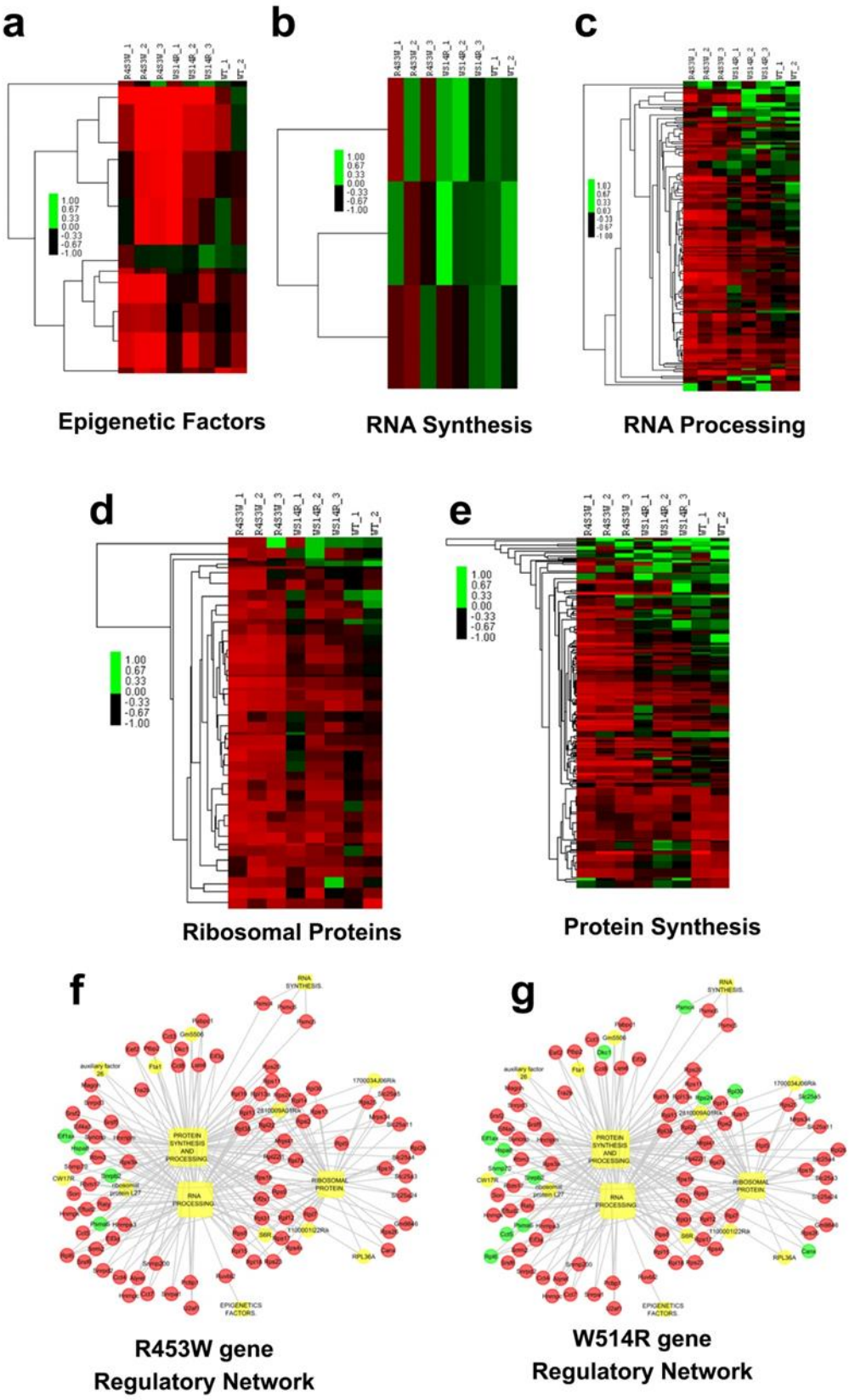

Figure 6 : Assessment of individual dysregulated GO categories related to gene expression regulatory process in mutants. (a), (b), (c), (d), (e) represent heatmaps of epigenetic

factors, RNA synthesis, RNA processing, ribosomal proteins, protein synthesis & processing . (f), (g) protein association clusters with proteins name in mutant samples, R453W LA and W514R LA respectively. Red color indicates upregulation and green color indicates down regulation.

Adam M et al. 2001 suggested, H2afz protein regulates the recruitment of RNA pol II enzyme on promoters of some genes and acts as important cofactor for expression of some genes .Interestingly, we observed high expression level of H2afz protein in mutants ,which has positive correlation with histone activating marks and exactly inverse with the level of H3K27me3 (Jeronima C et al. 2013) . We also found that mutants had a high level of expression of the Hist1h1d protein (**Figure. 7**), which has been linked to low H3K27me3 modification, according to Tiberi, Duprez et al. 2015. Their group showed enrichment in H3K27me3 level in Hist 1 locus using ChIP sequencing analysis, and high expression of HIST1 genes in the "low H3K27me3 level" group using qPCR analysis. Furthermore, we found high levels of HP1BP3 in R453W (**Figure. 7**), indicating the cessation of chromatin in a specific state, as Orly J et al.2015 discovered HP1BP3 co-localization with HP1 dots. Of note, changing of the balance of repressive and activating methylation is confirmed by the repressed expression of histone methylases for epigenetic marks : SET domain proteins in mutant cells. As an aside, from gene regulatory network we found, upregulation of the proteins involved in RNA synthesis, RNA processing, ribosomal proteins, protein synthesis etc. in mutants , which confers profound anomaly in the regulation of gene expression. Recent studies depicted some of hnRNPs and other splicing factors are connected with lamin A (Roux et al. 2012). Interestingly, we found hyper expression of members of heterogenous nuclear ribonucleoprotein (hnRNP) family in mutant cells, which are associated with pre-mRNA transcription, processing and their availability by other RNA processing factors(Kim et al. 2000, Martinez-Contreras et al. 2007).

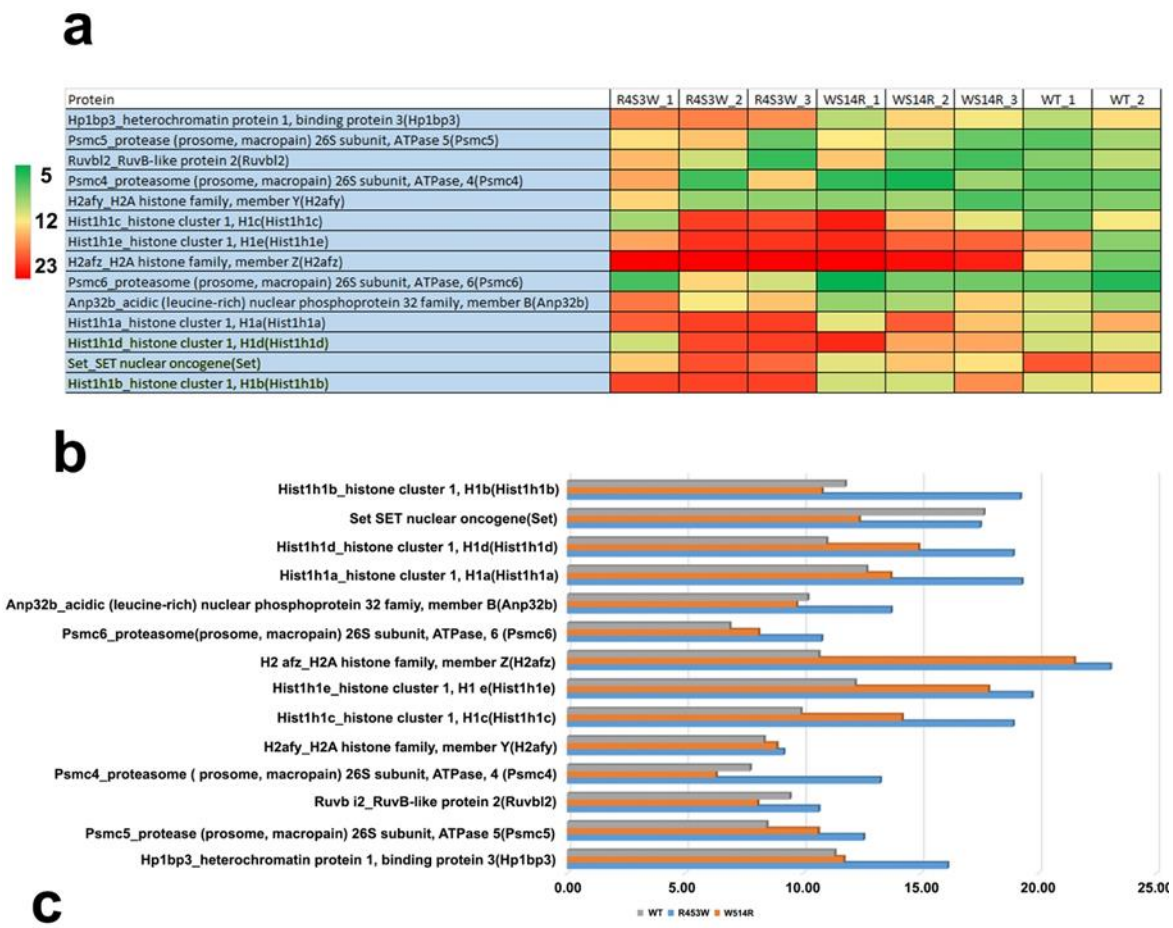

c

Genes	Gene Symbol	p value	Regulation	Fold change R453W vs Wt	p value	Regulation	Fold change W514R vs Wt
ENSMUSG00000037894	H2afz	0.00	up	4844.68	0.00	up	1756.23
ENSMUSG00000058773	Hist1h1b	0.00	up	172.95	0.72	up	1.64
ENSMUSG00000049539	Hist1h1a	0.00	up	71.78	0.45	up	3.21
ENSMUSG00000028759	Hp1bp3	0.01	up	28.68	0.89	up	1.18
ENSMUSG00000051627	Hist1h1e	0.05	up	62.94	0.01	up	86.19
ENSMUSG00000028333	Anp32b	0.06	up	15.96	0.80	up	1.38
ENSMUSG00000052565	Hist1h1d	0.09	up	39.99	0.01	up	52.34
ENSMUSG00000036181	Hist1h1c	0.09	up	65.58	0.05	up	46.70
ENSMUSG00000015937	H2afy	0.24	up	4.09	0.93	up	1.10
ENSMUSG00000054766	Set	0.54	down	-2.22	0.01	down	-38.13
ENSMUSG00000003868	Ruvbl2	0.67	up	1.98	0.98	up	1.03

Figure 7:

(a) Heatmap of epigenetic regulators within the replicates of 3 samples. (b) Absolute protein level comparison histograms of 3 samples.(c) List of differentially expressed epigenetic regulators in R453W mutant compared to WT LA, W514R mutant compared to WT LA.

Identification of changes in proteomic profiles that are associated with lamin protein:

Dittmer TA et al. 2014 tested 104 interactors by microscopy and yeast two hybrid screen assays and found 53% of interactors distributed in NE and 47% of interactors have been distributed

throughout the nucleus . So, understanding the levels of mutation specific lamin A interactors can be a reflection of disease specific accountability. We identified 65 lamin A interactors using STRING DB, where high proportion of proteins(49/65) have been scored unchanged. For R453W LA sample 16 proteins are found in upregulated list .However, 7 upregulated proteins and 9 downregulated proteins were detected in W514R LA sample **Table 2**. These include asymmetric expression patterns of emerin, lamin B1 and B2,Sun2 among the mutants, which are crucial interactors of lamin A for the maintenance of gene expression layer and structure of chromatin (May CK et al. 2018, Koch AJ et al.2012,Pascual-reguant L et al. 2018, Ma Y et al. 2017).

Table 2 : List of differentially expressed protein interactors in R453W mutant compared to WT LA, W514R mutant compared to WT LA.

Uniprot ID	Entrez Gene ID	Protein Symbol	Protein Name	Regulation R Vs WT	FC R Vs WT	p W vs WT	Regulation W vs WT	FC W vs WT
EMD_MOUSE	13726	Emd	emerin	up	14.21	0.24	down	-5.30
A0A087WS56_MOUSE	14268	Fn1	fibronectin 1	up	13.61	0.98	down	-1.03
A0A0H2UH27_MOUSE	14359	Fxr1	fragile X mental retardation gene 1, autosomal homolog	up	30.41	0.10	up	9.99
LMNB1_MOUSE	16906	Lmnb1	lamin B1	up	13.01	0.86	up	1.30
A0A0R4J0Q5_MOUSE	16907	Lmnb2	lamin B2	up	6.58	0.68	down	-1.62
A0A0R4J1N9_MOUSE	21780	Tfam	transcription factor A, mitochondrial	up	16.45	0.32	up	3.45
Q0V930_MOUSE	21894	Tln1	talin 1	up	182.19	0.11	up	31.96
LAP2B_MOUSE	21917	Tmpo	thymopoietin	up	455.21	0.01	up	37.40
VINC_MOUSE	22330	Vcl	vinculin	up	5.00	0.29	down	-4.94
PEBP1_MOUSE	23980	Pebp1	phosphatidylethanolamine binding protein 1	up	5.10	0.76	down	-1.43
Q05CQ4_MOUSE	29875	Iqgap1	IQ motif containing GTPase activating protein 1	up	40.42	0.37	down	-3.09
A2A5N2_MOUSE	54401	Ywhab	tyrosine 3-monooxygenase/tryptophan 5-monooxygenase activation protein, beta polypeptide	up	40.21	0.12	up	7.36
SND1_MOUSE	56463	Snd1	staphylococcal nuclease and tudor domain containing 1	up	17.81	0.89	down	-1.18
CDC5L_MOUSE	71702	Cdc5l	cell division cycle 5-like (S. pombe)	up	3.85	0.44	down	-2.84
E0CY44_MOUSE	223697	Sun2	Sad1 and UNC84 domain containing 2	up	67.25	0.68	down	-1.69
D3Z3Y3_MOUSE	381760	Ssbp1	single-stranded DNA binding protein 1	up	13.24	0.53	up	2.12

Discussion:

The nuclear membrane plays a critical role in chromosome organization through a variety of protein-protein interactions, as well as maintaining the peripheral and nucleoplasmic heterochromatin pools (Zuleger et al. 2011,2013). Mattout et al. (2011) previously reported that heterochromatin is heavily involved in the disease mechanism caused by lamin A mutations. Lamins are thought to be associated with chromatin through histones and DNA (Kind and van Steensel 2010). Histone modifications are presented as paradigmatic signatures in gene expression and regulation (Gibney and Nolan, 2010). High levels of H3K9me3,

HP1and higher dynamics reveal constitutive heterochromatin signatures (Trojer and Reinberg, 2007). H3K9me3 and HP1 marks, as well as their dynamics are dramatically reduced in mutants used in this study, indicating a less condensed state of chromatin, which could lead to increased transcription activity. In addition, immunofluorescence and immunoblotting studies revealed a significant decrease in H3K27me3 levels and an increase in H3K36me3. There are some caveats, however, regarding the roles of H3K27me3 and H3K36me3. H3K27me3 is usually associated with transcription repression, but the enrichment of H3K27me3 around transcriptional start site (TSS) genes could indicate that H3K27me3 has a dual role (Young et al. 2011, Shah et al. 2013). H3K36me3 is also linked to heterochromatin, both constitutive and facultative (Chantalat et al. 2011). Furthermore, we discovered the increased expression of Hist1h1d from the proteomics dataset. Hist1h1d expression is negatively correlated with H3K27me3 modification level, according to Tiberi, Duprez et al. 2015. In HGPS cells, Scaffidi and Misteli (2006) and Shumaker et al. (2006) found a decrease in H3K9me3 levels and an increase in H4K20me3 levels. The modulation of transcription initiation sites can be regulated by the interaction of epigenetic DNA and histone modifications (Quina A. S., Di Croce L.2006). Accordingly, from immunoblot results we identified a high level of RNA Pol II recruitment, which could lead to proactive transcription initiation. Surprisingly, proteomics results revealed that regulatory proteins for the RNA polymerase II transcriptional preinitiation complex were expressed at higher levels. As a result, we can conclude that lamin A modulates epigenetic landscape, which may cause or contribute to disease pathogenesis molecular mechanisms.

According to Bank et al. 2011 and Bertrand et al. 2012, the LMNA delK32 mutation is linked to severe early-onset congenital muscular dystrophy. It results in defective lamin assembly as well as complete loss of lamin from the periphery of the nucleus. In HGPS cells, expression of truncated Lamin A/progerin causes H3K9me3, H3K27me3 , HP1 loss and a reduction in the peripheral hetrochromatin pool (Misteli et al. 2006, Giordano et al. 2014, Lattanzi et al. 2005. Gasser et al.2011 discovered that retention of muscle-specific promoters at the perinuclear sight altered expression of muscle-specific genes. To connect our findings to the gene expression hypothesis, we can speculate that muscular dystrophy mutations cause lamin A to be pulled into the nuclear interior rather than the periphery of the nucleus, causing a vehement perturbation of the complex of lamin A-lamin binding proteins-chromatin in the periphery and, as a result, changes in the overall chromatin mechanism. This would also imply that the localization of nuclear membrane proteins at inner nuclear membrane is based on their

binding to lamins (Ostlund C et al. 2001) . Consequently, we found precipitation of epigenetic marks in nuclear foci of the two mutations. It has been reported that, crucial nuclear envelope protein Emerin interacts directly with some chromatin-modifying enzymes (Holaska JM et al. 2007) , which probably accounts for the increasing fraction of epigenetic marks being precipitated here. Though, further studies are required to determine how the regulation of the interactions between these components may be the underlying cause of rejig of chromatin states in lamin A associated muscular dystrophies.

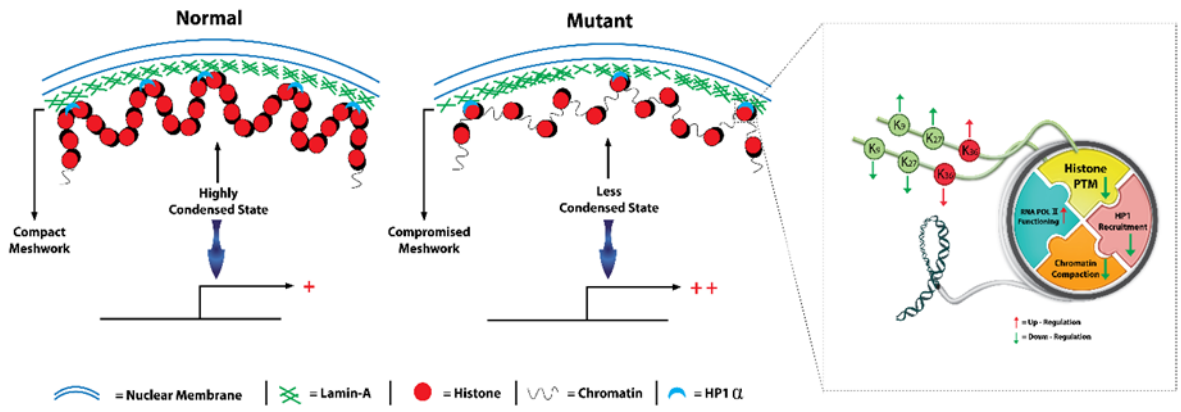

Figure : Schematic diagram representing the results. Mutations in lamin A protein evicts the nucleosome from nuclear periphery and consequently promotes aberrant gene expression.

These distinct change in the attachment sites and expression patterns might have resulted from the structural ambiguity of lamin A protein due to two different point mutations in Ig fold domain. Interestingly, our previous studies depicted dissimilar electrostatic surface potential among the mutants and lower binding affinity towards some important nuclear envelope proteins. W514R mutation possesses electropositive surface potential in the Ig fold domain, where as R453W mutation attributes to electronegative surface potential. In this report, we have gained novel insight into the structure of both of the mutants. Our results from the rheology experiment demonstrate a function of polymer concentration acts as a rich repertoire in promoting different binding strength of protein. Jamming behavior of W514R and unjamming behavior of R453W LA disturbed their load bearing capacity into two different ways.This observation supports the notion that, re-establishing of chromatin interactions with nuclear envelope happens if lamin intermediate filament acts as a “brick and mortar scaffolding”.In this case, nuclear rupture occurs with the mess up of particular patterns of

spatial genome organization due to extracellular forces that translates to nucleus through cytoskeleton and inner nuclear forces by chromatin as well(Zulegar N et al. 2011).Our observations from SEM images in in vitro condition also pointed to a difference in network organization between the wild type and the mutants. We performed CD spectroscopy experiments to seek support in favour of our SEM images. The CD spectra of mutants confirmed change in the secondary structure of overall protein.W514R LA more or less fitted into canonical coiled coils. Tail domain of lamin A carries positive charge , which helps in crosslinking within the coiled-coil segments to assign a spring like behaviour in entire rod domain. So, we can extrapolate further that the more positive charge generated by W514R mutation inhibits all the flexible regions of the lamins and may result in increased bundling but relatively lower cross-link density in network compared to wt LA as observed from SEM images.On the other hand, the R453W mutation destabilizes the Ig fold domain by removing a salt bridge and thus we observed loose network formation by this mutant protein.

Furthermore, we observed upregulation of proteins of RNA synthesis, RNA processing, ribosomal proteins, protein synthesis & processing, which may be associated with aberrant splicing, translation, and processing in lamin A associated muscular dystrophy, is consistent with the above findings. This finding could support the idea that the steps in gene transcription leading to upstream and downstream translation events, are intertwined. It also shows good agreement with Viera et al.2014, which showed upregulation of protein translation and RNA processing/splicing in limb–girdle muscular dystrophy. Kong et al.2010 found altered splicing of some sarcomeric genes, such as troponin T2, troponin 13, myosin heavy chain 7, and filamin C gamma, which are important biomarkers in DCM and hypertrophied myocardium, respectively. Finally, our findings could point to a link between different types of myopathies caused by faulty RNA and protein processing.

Methods:

Site directed mutagenesis:

Site directed mutagenesis was performed on pEGFP –human lamin A (gift from Dr. Robert D. Goldman, Northwestern University, Chicago) following the protocol as decribed in (Bhattacharjee et al. 2013) to obtain the mutations R453W, W514R. Primer sets each containing the mutations are :

R453W-sense 5’-GGAGGGCAAGTTTGTCTGGCTGCGCAACAA-3’, R453W-antisense 5’- TTGTTGCGCAGCCAGACAAACTTGCCCTCC- 3’, W514R-sense 5’-

CTAACCGACCTGGTGAGGAAGGCACAGAAC - 3', W514R-antisense 5'-GTTCTGTGCCTTCCTCACCAGGTCGGTAG - 3'. Mutants were confirmed by Sanger sequencing .

Stable cell line preparation:

Mouse myoblast cell line C2C12 was first transfected with EGFP-Wt LA, EGFP-R453W LA, EGFP-W514R LA using Lipofectamine 2000 . C2C12 stable cell line were prepared for EGFP-WT LA, EGFP R453W, EGFP W514R using 850 μg of G418 and used in entire cell biology experiments.

Immunofluorescence analysis:

Stably transfected mouse myoblast C2C12 cells either grown on 18*18 mm cover glasses were fixed using 4% PFA for 10 min, followed by PBS wash. Cells were permeabilized by 0.2% Triton X-100 solution in PBS stained with antibody anti-Histone H3(tri methyl K27) [Active Motif ; 39155], anti-Histone H3 (tri methyl K9) [Active Motif; 39161], anti-histone (tri methyl K36) [Abcam; ab9050] , anti- HP1 alpha [Abcam ;ab234085] of 1:1500 dilution for overnight at 4° C temperature. Then cells were incubated with secondary antibody, Alexa 594 conjugate Invitrogen (A11005) for 2 hour at RT. Finally, coverslips were mounted on Vectashield (Vector laboratories) for imaging.

Image Acquisition:

The slides were visualized in NIKON Inverted Research Eclipse TiE Laser Scanning Confocal/NSIM microscope. Confocal images were captured by Galvano mode NIKON A1 RMP detector and Plan Apochromat VC 100x oil DIC N2 / 1.40 135 NA /1.515 RI objective with an additional 4x digital zoom . A multi line Argon -Krypton laser (λ_{ex}- 457/488/561 nm) at 3% was used for green channel and a solid state laser (λ_{ex}-561 nm) at 5% was used for red channel . For Z stacks a step size of 0.25 μm was maintained. 25 cells per sample were checked for the study. Every sample was tested for three independent experiments. Images were processed using Ni Elements Analysis Ver 4.13.

Flouorescence recovery after photo bleaching (FRAP) :

C2C12 cells were grown on Nunc Glass Bottom Dish, 27 mm (Cat no.150682) in High Glucose Dulbecco's modified Eagle medium (DMEM) (Gibco), complemented with 10% fetalbovine serum (Gibco) and 1% penicillin-streptomycin (Gibco), in a humidified incubator at 37ºC in

5% CO2. Cells were synchronized at G2/M phase with 200 ng/ml nocodazole (Sigma) for 12 hrs (Tintignac LA et al. 2004). Cells were washed three times with PBS and replenished with pre-warmed fresh complete media after release form the block. After 3hrs from release of the nocodazole block cells were double transfected with pEGFP-human LA (EGFP-wt LA and mutants) and RFP-HP1α using Lipofectamine 2000 (Invitrogen) in accordance with the manufacturer's protocol at early passages having 60-70% confluency and were kept in culture for 24 hrs.

FRAP experiments were performed on a Nikon Inverted Research Eclipse TiE Laser Scanning Confocal/NSIM microscope. A 2μm × 2μm region at the nuclear periphery in the mid-focal plane was bleached at 100 % power of the argon laser (405 nm) running at 40.6 mw. The pinhole size for the confocal was set at 1 Airy unit. Bleaching was done for 5s followed by 50s for recovery. 30 cells per sample was selected for FRAP analysis from at least 2 independent experiments . Immediately, following the bleach , images in the Z plane were captured . The best Z-plane image for the bleached ROI was selected from each time point 3D stack to avoid cell movement, nuclear rotation and focus drift to register the bleach ROI between time points. Cells were maintained at 37°C,5% CO_2 using a steam incubator. Data was normalized as reported by Dundr et al. 2002, Phair et al. 2004 using following equation :

$$F_{Data}\ (t))/F_i$$

$F_{Data}(t)$ = Back ground corrected FRAP data at specific time point.

F_i = Prebleach steady state fluorescence.

We have used following equations to calculate the halftime ($t_{1/2}$) of recovery and mobility fraction(M_f) :

$$t_{1/2} = \frac{F\infty + F0}{2} \ldots \text{(i)}$$

$$M_f = \frac{(F\infty - F0)}{(Fi - F0)} \times 100 \quad \ldots \text{(ii)}$$

Immunoblotting :

Stably transfected cells were harvested after rinsing off the media with 1x PBS. Cells were lysed in RIPA buffer with 7M Urea (50mM Tris-HCL pH 8.0, 150 mM NaCl, 0.75% SDS (w/v), 0.5% Sodium Deoxycholate (w/v), 1% Triton X-100 (v/v), on ice for 30 min followed by sonication with UP200S Ultra Schallprozessor at 0.5 cycles ,amplitude set at 60-70% to

lyse the cells until the solution become transparent. Cell lysate was mixed with chilled acetone at 1: 3 ratio and kept for overnight at -20° C. On the next day cell pellet was achieved by centrifugation at 13000 rpm for 10 min and resuspended in RIPA buffer with 7M Urea. After protein estimation by Bradford reagent using Nanodrop 2000 spectrophotometer (Thermo scientific) and equal amounts of protein (35 μg)were loaded and resolved on 15% SDS PAGE. Proteins were transferred to nitrocellulose membrane, and probed as with primary (overnight at 4 °C) and secondary antibodies (2 h at RT), Following antibodies were used :

Antibody	Source	Catalog number	Dilution
Histone H3 (tri methyl K9)	Active Motif	39161	1:1000
Histone H3 (tri methyl K27)	Active Motif	39155	1:1000
Histone H3 (tri methyl K36)	Abcam	ab9050	1: 1000
HP1 alpha	Abcam	ab234085	1:800
RNA polymerase II CTD (4H8)	Abcam	ab5408	1: 1000
β Actin	Sigma–Aldrich	A5316	1:800

Super Signal West Pico Chemiluminescent Substrate (Thermo Scientific) was used to develop chemiluminscence and imaged using Kodak Medical X-ray Films. Blots were repeated in triplicates if not otherwise mentioned. Quantifications from the blots were performed using Image J software. Data presented as bar diagrams by normalizing the intensity of histone modification marks, RNA Pol II S5p marks with loading control actin .

LC-MS/MS :

20 μg of protein per sample from three biological replicates per treatment group and two from control was taken for analysis. Sample were alkylated in dark for 20 mins at RT with 30 mM Iodoacetamide following reduction with 10m mM DTT at 56 ° C for 30 mins. pH of the solution was adjusted to 8 by adding 25 mM of ammonium bicarbonate. Then trypsin (0.2 μg/μL) was

added to the solution so that the concentration of trypsin: proteins was 1: 50. After trypsin addition, the samples were incubated overnight at 37° C. 5 % formic acid was added to stop the reaction. Chromatographic separation was achieved on Pep map TM 100(75μmx * 2 cm); Nanoviper C 18, (3 μm; 100 A°) as precolumn and EASY SPRAY PEPMAP RSLC C18 2 μM (50 cm * 75 μm;100 A°) as analytical column . .4 μg sample was injected onto column. The mobile phase A was 0.1% Formic acid in MS grade water and mobile phase B was 80% Acetonitrile + 0.1% formic acid in MS grade water . Step gradient Mobile phase B was used from 10% to 95% for 3 hr with 300 μL/min flow rate. A survey full scan MS (from m/z 375-1700) was acquired in the Orbitrap Fusion detector with a resolution of 120000. MS/MS was performed with a scan range m/z 100-2000 in the Ion trap detector. Protein identification was performed by searching MS/MS data against the swiss-prot mouse protein database downloaded on Oct 2, 2018 using the in house mascot 2.6.2 (Matrix Science) search engine. The search was set up for full tryptic peptides with a maximum of two missed cleavage sites. Acetylation of protein N-terminus and oxidized methionine were included as variable modifications and carbamidomethylation of cysteine was set as fixed modification. The precursor mass tolerance threshold was set 10 ppm for and maximum fragment mass error was 0.02 Da. The significance threshold of the ion score was calculated based on a false discovery rate of ≤ 1%. Qualitative analysis was performed using progenesis QI proteomics 4.1 (Nonlinear Dynamics).

Statistical Analysis :

Data are presented as means ± SD. The entire significance test for immunofluorescence and immunoblot assays were obtained using student's t-test . $P < 0.05$ was considered statistically significant.All the experiments were repeated for three times. Origin (OriginLab, Northampton, MA) was used for all FRAP analysis.

Expression and purification of protein:

Full length human lamin A protein/pre-lamin A (664 amino acids) used for this study was expressed from pET-LA, transformed into BL21(DE3)pLysS competent cells and cultured in TB broth (Himedia, Mumbai, India) in the presence of penicillin and chloramphenicol (USB corporation, Cleveland, OH, USA). Protein expression was induced with 2 mM IPTG (Himedia, Mumbai, India) for 2 hours. Cell lysate was prepared as described by Moir et.al. 1991 and separated on a Mono STM5/50 GL Column (GE Healthcare, Uppsala, Sweden) fractions were eluted in 6 M urea, 25 mM TrisHCl pH 8.6, 250 mM NaCl and 1 mM DTT

(Urea buffer). Using Slide –A-Lyzer –Minidialysis units with a 10,000 Dalton MWCO(Thermo Scientific, Rockford, IL, USA) proteins were renatured by dialyzing out urea in a step wise manner from 6 M in steps of two at room temperature. 25 mM Tris-HCl buffer of pH 8.6 with 250 mM NaCl and 1 mM DTT, has been used for all experiments with the wild type and mutant proteins. Protein concentrations were determined by standard Bradford reagent (Bio-Rad, Hercules, CA, USA) in a Perkin Elmer Luminiscence Spectrometer. Deionised water of highest purity (Resistivity18.2 MV.cm 25°C) obtained from Synergy Millipore water purification system was used for preparing the buffers.

Scanning Electron Microscopy (SEM) :

Renatured protein samples that are in 25 mM Tris-HCl buffer of pH 8.6 with 250 mM NaCl and 1 mM DTT were spotted on circular coverslips (F-13mm), dried in vacuum and coated with gold in IB2 Iron Coater. Samples were imaged in Hitachi S530 Scanning Electron Microscope (Japan) by 3000x magnifications at 25 kV.

Rheological measurements :

The cone and plate rheological measurements were carried out in a stress controlled rheometer (MCR 502, Anton Paar, Graz, Austria) operated through a software (Rheoplus/ 32,service V.3.61). The lower plate is fixed and the shear deformations were applied by rotating the upper cone with a 25 mm diameter, 2°cone -and-plate fixture in a controlled manner. The amplitude (γ) was kept in 1% and angular frequency (ω) was kept in 5 rad/sec..6 mg/ml of Wild type and mutant proteins in buffer were loaded between the cone-plate and the temperature was maintained at 20°C by Peltier control system. The protein samples were placed in a humidified chamber (with buffer solution) during the measurements, to prevent evaporation of the solvent. The measurements were adequately repeated for 100 measurement points with a duration of 10sec.

Circular Dichroism (CD) Spectroscopy:

Far-UV CD spectra of 4 µM full length human lamin A protein were recorded at 25°C in a Jasco J-720 Spectropolarimeter with a quartz cuvette having a path length of 1 mm. CD spectroscopy were recorded in the far UV range of 200-250 nm at 25°C,with data collected in a continuous mode with a 1nm bandwidth and scan speed of 10 nm/min. Properly refolded proteins were examined after extensive dialysis in 4 M, 2 M urea buffer and finally in the working buffer separately. The spectrum of working buffer at 25°C (average of 10 scans) were

subtracted from each spectrum. The molar ellipticity (ME) in deg cm^2 $dmol^{-1}$ was calculated, using following equation :

ME (deg cm^2 $dmol^{-1}$) $= \frac{\theta \times 10^{\wedge}\mathbf{6}}{d \times c}$

θ is the ellipticity in mdeg, d is the path length in nm and c the protein concentration in µM.

Acknowledgments:

The authors thank Dr. Dipayan Sanyal (CSIR-CGCRI) ,Dr. Srikanta Chakraborty(University of Burdwan) for sharing of equipments and insightful discussion. For LC-MS/MS authors acknowledge Biologics Characterization Facility, C-CAMP. We thank Dr. Prabal Chakraborty , application Scientist , Towa Optics India Pvt Ltd. for valuable inputs regarding image processing. This research was partly funded by SERB-DST and BARD project,DAE.

Author Contributions:

S.D.,M.V. conceived and designed the experiments. SD Performed all the immunofluorescence and immunoblot studies, biophysical experiments . S.D. , M.V. and V.K. analysed the proteomics data. S.D., M.V.,V.K. made the draft of the manuscript. All authors have read and agreed to the published version of the manuscript.

References :

1.Dechat ,T, Pfleghaar K, Sengupta K, Shimi T,Shumaker D, Solimando L, Goldman R. Nuclear lamins : major factors in the structurl organization and function of the nucleus and chromatin . 2008; genes dev. 2008, 22(7): 832-853.

2.Malhas ,B.M., Lee ,C.F., Sanders,R., Saunders, N.J. and Vaux,D.J. Defects in lamin B1 expression or processing affect interphase chromosome position and gene expression. 2007; J Cell Biol. 176,593-603.

3.Tang C.W., Maya-mendoza A., Martin C., Zeng K.,Chen S., ferret D., Wilson S.A., Jackson D.A. The integrity of a lamin –B1 dependent nucleoskeleton is a fundamental determinant of RNA seyntesis in human cells. J. Cell. Sci.2008.121: 1014-1024.

4.Schirmer and Foisner , Proteins that associate with lamins : many faces,many functions. Exp Cell Res.2007. 10;313(10): 2167-79.

5.Filesi et al . Alterations of nuclear envelope and chromatin organization of

In mandibuloacral dysplasia , a rare form of laminopathy.physiol. Genomics , 2005 .23,pp.150-158

6.Galiova G, Bartova E, Raska I, Krejci J, Kozubek S. Chromatin changes induced by lamin A/C deficiency and the histone deacetylase inhibitor trichostatin A. Eur J Cell Biol. 2008.87:291-303

7.Gonzalez Suarez I, Redwood A B, Perkins S M, Vermolen B, Lichtensztejin D, Grotsky D, Palacin L M, Gapud E J, Sleckman B P, Sullivan T, Sage J, Stewart C L, Mai S, Gonzalo S. Novel roles for A type lamins in telomere biology and the DNA damage response pathway. EMBO J.2009 28(16) : 2414-27.

8.Goldman RD, Shumaker DK , Erdos MR, Eriksson M, Goldman AE, Gordon LB, Gruenbaum Y, Khuon S, Mendez M, Varga R. Accumulation of mutant lamin A causes progressive changes in Hutchinson –Gilford progeria syndrome. Proc Natl Acad Sci USA ,2004. 101 : 8963-8;PMID : 15184648 .

9. Adam M, Robert F, Larchelle M and Gaudreau L. H2A.Z is required for global chromatin integrity and for recruitment of RNA polymerase II under specific conditions. Mol. Cell. Biol. 2001. 21, 6270-6279.

10.Tiberi G, Pekowaska A, Oudin C, Ivey A, Autret A, Prebet T, Koubi M, Lembo F, Mozziconacci M-J, Bidaut G, Chabannon C, Grimwade D, Vey N, Spicuglia S, Calmes B, Duprez E. PcG methylation of the HIST 1 cluster defines an epigenetic marker of acute myeloid leukemia. 2015.29(5) : 1202-6

11.Lattanzi G,Columbaro M, Elisabett M, Cenni V, Camozzi D, Wehnert M, Santi S, Riccio M, Coco RD, Maraldi NM, Squarzoni S, Foisner R, Capanni C . journal of cellular biochemistry.2007, 10.1002/jcb.21467

12.Scaffidi P ,Misteli T. lamin A dependent nuclear defects in human aging. Science. 2006. 312(5776) : 1059-63

13.Shumaker et al. Mutant nuclear lamin A leads to progressive alterations of epigenetic control in premature aging. Proc Natl Acad Sci USA .2006,10.1073/pnas.0602569103

14.Kouzarides T . Chromatin modifications and their function. Cell . 2007.02.005

Bartova E,Krejci J, Harnicarova A, Galiova G, Kozubek S. Histone modifications and nuclear architecture : A review. J Histochem Cytochem .2008.56(8): 711-721.

15.Berger SL . The complex language of chromatin regulation during transcription. Nature. 2007 .447(7143): 407-12

16.RoblekM, Schuchner S, Huber V,Ollram K, S Vlcek-Vesely, Foisner R, Wehnert M, Ogris E. Monoclonal antibodies specific for disease associated point mutants : Lamin A/C R453W and R482W. 2010. Plos ONE 5(5) : e 10604.

17.Dutta S, Das J K, Maganti L, Bhattacharyya M, Bhattacharyya D, Mukherjee S & Sengupta K. Skeletal muscle dystrophy mutant of lamin A alters the structure and dynamics of the Ig fold domain.Scientific Reports .2018. 8, 13793

18.Trojer P, Reinberg D. Facultative heterochromatin : is there a distinctive molecular signature ?. Mol Cell. 2007. 28(1):1-13

19.Chaturvedi P, Parnaik VK. Lamin A rod domain mutants target heterochromatin protein 1α and β for proteasomal degradation by activation of F-Box protein ,FBXW10. Plos one. 2010. 5(5):e10620

20.R D. Goldman, Gruenbaum Y, Moir RD, Shumaker DK, Spann T. Nuclear lamins : building blocks of nuclear architecture . Genes Dev. 2002. 16(5):533-47.

21.Kumaran RI, Thakar R, Spector DL. Chromatin dynamics and gene positioning. Cell.2002. 132 (6) : 929-934

22.Hessen S ,Fornerod M.The nuclear envelope as a transcription factor resting place.EMBO reports. 2007.8:914-919.

23.Chapman RD et al. molecular evolution of the RNA polymerase II CTD.Trends Genet.2008.24(6):289-96.

24.Zuleger N,Boyle S, Kelly DA. Heras J, Lazou V, Korfali N, Batrakou D, Randles K N, Morris G E,Harrison DJ, Bickmore W, Schirmer E C . Genome Biology 14 .R14.(2013).

25.Zuleger N, Kelly DA., Richardson A C, Kerr A R W,Goldberg M W,Goryachev A B, Schirmer E C. system analysis shows distinct mechanisms and common principles of nuclear envelope protein dynamics.J Cell Biol. 2011.193(1): 109-23.

26.Mattout A, Pike BL, Towbin BD, Bank EM, Sandoval G, Stadler MB, Meister P,Gruenbaum Y,Gasser SM . An EDMD mutation in C.elegans lamin blocks muscle –specific gene relocation and compromises muscle integrity.Curr Biol. 2011.21, 1603-14.

27.Kind J, Steensel BV. Genome- nuclear lamina interactions and gene regulation.Curr opin Cell Biol. 2010. 22(3): 320-5

28.Gibney E R, Nolan C M. Epigenetics and gene expression. Heredity (Edinb) .2010. 105(1) : 4-13.

29.Trojer P , Reinberg D. facultative heterochromatin : is there a distinctive molecular signature ? . Mol Cell. 2007. 28(1):1-13.

30.Young M D, Wilson T A, Wakefield M J, Trounson E, Hilton D J, Blewitt M E, Oshlack A, Majewski I . ChIP-seq analysis reveals distinct H3K27me3 profiles that correlate with transcriptional activity.Nucleic Acids Research. 201139(17): 7415-7427.

31.Shah P P, Donahue G, Otte G L, Capell B C, Nelson D M, Cao K, Aggarwala V, Cruickshanks H A, Rai T S,McBryan T, Gregory B D, Adams P D , Berger S L .

Lamin B1 depletion in senescent cells triggers large-scale changes in gene expression and the chromatin landscape.Genes Dev. 2013. 27(16):1787-99.

32.Chantalat S, Depaux A,Hery P, Barral S, Thuret J Y, Dimitrov S, Gerard M. Histone H3 trimethylation at lysine 36 is associated with constitutive and facultative heterochromatin. Genome Res. 2011 .21(9):1426-37.

33.Shumaker D K, Dechat T, Kohlmaier A, Adam S A, Bozovsky M R, Erdos M r, Eriksson M, Goldman A E, Khuon S, Collins F S, Jenuwein T, Goldman R D. mutant nuclear lamin A leads to progressive alterations of epigenetic control in premature aging. Proc Natl Acad Sci USA. 2006 .103(23):8703-8.

34.Quina A. S. , Buschbeck M,Di Croce L. chromatin structure and epigenetics . Publons.2006.06.016.

35.Viera N M, Naslavsky M S, licinio L, Kok F, Schlesinger D, Vainzof M, Sanchez N, Kitajima J P,Gal L, Cavacana N, Serafini P R, Chuartzman S, Vasquez C, Mimbacas A, Nigro V, Pavanello R C, Schuldiner M , kunkel L M, Zatz M .A defect in the RNA –processing protein HNRPDL causes limb-girdle muscular dystrophy 1G(LGMD1G). Hum Mol Genet.2014.23(15): 4103-10

36.Moir, R. D., Yoon, M., Khuon, S. & Goldman, R. D. Nuclear lamins A and B1: different pathways of assembly during nuclear envelope formation in living cells. *J. Cell Biol.* **151**, 1155–1168 (2000).

37.Melcer, S. et al. Histone modifications and lamin A regulate chromatin protein dynamics in early embryonic stem cell differentiation. *Nat. Commun.* **3**, 910 (2012).

38.Prokocimer, M. et al. Nuclear lamins: key regulators of nuclear structure and activities. *J. Cell. Mol. Med.* **13**, 1059–1085 (2009).

39.McCracken, S., Fong, N., Yankulov, K., Ballantyne, S., Pan, G., Greenblatt, J., Patterson, S. D., Wickens, M., and Bentley, D. L. 1997 The C-terminal domain of RNA polymerase II couples mRNA processing to transcription. *Nature (London)* **385**, 357– 361

40.Shuman, S. 1997 Origins of mRNAidentity: capping enzymes bind to the phosphorylated C-terminal domain of the RNA polymerase II. *Proc. Natl. Acad. Sci. USA* **94**, 12758– 12760

41.Hirose, Y., and Manley, J. L. 1998 RNA polymerase II is an essential mRNA polyadenylation factor. *Nature (London)* **395**, 93– 96

42. L.A. Tintignac, V. Sirri, M.P. Leibovitch, Y. Lécluse, M. Castedo, D. Metivier, G. Kroemer, S.A. Leibovitch, Mutant MyoD lacking Cdc2 phosphorylation sites delays M-phase entry, Molecular and cellular biology 24 (2004) 1809-1821.

43. T. Kouzarides, Chromatin modifications and their function, Cell 128 (2007) 693- 705.

44. Heitlinger E., Peter M., Lustig A., Villiger W., Nigg E.A., Aebi U. (1992) The role of the head and tail domain in lamin structure and assembly: analysis of bacterially expressed chicken lamin A and truncated B2 lamins. J Struct Biol, 108, 74–89.

45. Isobe K., Gohara R., Ueda T., Takasaki Y., Ando S. (2007) The last twenty residues in the head domain of mouse lamin A contain important structural elements for formation of head-to-tail polymers in vitro. Biosci. Biotechnol. Biochem., 71, 1252–1259.

46.Adam, S.A.; Butin-Israeli, V.; Cleland, M.M.; Shimi, T.; Goldman, R.D. Disruption of lamin B1 and lamin B2 processing and localization by farnesyltransferase inhibitors. Nucleus 2013, 4, 142–150.

47.Maske, C.P.; Hollinshead, M.S.; Higbee, N.C.; Bergo, M.O.; Young, S.G.; Vaux, D.J. A carboxyl-terminal interaction of lamin B1 is dependent on the CAAX endoprotease Rce1 and carboxymethylation. J. Cell Biol. 2003, 162, 1223–1232.

48. Dominici, S.; Fiori, V.; Magnani, M.; Capanni, C.; Camozzi, D.; D'Apice, M.R.; Le Dour, C.; Auclair, M.; Caron, M.; Novelli, G.; et al. Different prelamin A forms accumulate in human fibroblasts: A study in experimental models and progeria. Eur. J. Histochem. 2009, 53, 43–52.

49.Corrigan, D.P.; Kuszczak, D.; Rusinol, A.E.; Thewke, D.P.; Hrycyna, C.A.; Michaelis, S.; Sinensky, M.S. Prelamin A endoproteolytic processing in vitro by recombinant Zmpste24. Biochem J. 2005, 387, 129–138.

50. Sinensky, M.; Fantle, K.; Trujillo, M.; McLain, T.; Kupfer, A.; Dalton, M. The processing pathway of prelamin A. J. Cell Sci. 1994, 107, 61–67.

51. Furukawa, K.; Inagaki, H.; Hotta, Y. Identification and cloning of an mRNA coding for a germ cell-specific A-type lamin in mice. Exp. Cell Res. 1994, 212, 426–430.

52.Dhe-Paganon, S.; Werner, E.D.; Chi, Y.I.; Shoelson, S.E. Structure of the globular tail of nuclear lamin. J. Biol. Chem. 2002, 277, 17381–17384.

53. Mukherjee C, Kundu A, Dey R, Banerjee A, Sengupta K. Active microrheology using pulsed optical tweezers to probe viscoelasticity of lamin A. Soft Matter. 2021 Jul 21;17(28):6787-6796. doi: 10.1039/d1sm00293g. PMID: 34219136.